

# Nonspherical dented poly(methyl methacrylate)/poly(styrene-co-divinylbenzene) particles formed in seeded soap-free emulsion copolymerization

Shan Shi · Tao Wang · Lina Bian · Limin Zhou ·  
Liqun Zhao · Shin-ichi Kuroda

Received: 17 April 2011 / Accepted: 31 May 2011 / Published online: 11 June 2011  
© Springer Science+Business Media, LLC 2011

**Abstract** In this study, nonspherical poly(methyl methacrylate)/poly(styrene-co-divinylbenzene) [PMMA/P(St-co-DVB)] particles having multiple dents on the surface were prepared by seeded soap-free emulsion copolymerization of St and DVB (used as a crosslinker) on spherical linear PMMA seed particles. The effect of various polymerization parameters on particle morphology, as well as polymerization kinetics and morphological evolution, were investigated in detail. It was found that, to prepare this kind of nonspherical particles, it was necessary to conduct the polymerization at a relatively low temperature, using batch monomer addition mode and PMMA seed of relatively high molecular weight. The formation of the nonspherical particles was attributed to the phase separation between the second-stage monomers and the crosslinked P(St-co-DVB) network being formed during polymerization.

## Introduction

Emulsion and dispersion polymerizations always tend to produce the polymer particles with perfectly spherical shape as a result of the minimization of surface tension [1–3]. Accordingly, it is difficult to directly synthesize polymer particles with nonspherical shape [4, 5] by these

methods. While, it was reported that nonspherical particles with a single indentation on them were formed in the course of the soap-free emulsion polymerization of styrene (St), these particles eventually became spherical at the end of the reaction [6]. On the other hand, crosslinking of the seed latex particles, in seeded emulsion or dispersion polymerization, is often done to impart specific physical properties to the final product [7]. Owing to the strong elastic force within the crosslinked seed particles, the surface tension is quite easily relegated to play a secondary role in determining the surface morphology. This allows for the preparation of nonspherical polymer particles under some conditions. For example, pre-swelling of the cross-linked seed particles with the second-stage monomer and subsequent polymerization usually led to the phase separation of the monomer from the crosslinked network, forming single or multiple new domains appended on the original seed particles. This technique has been applied to design and synthesize a wide variety of nonspherical particles having different surface morphologies. These nonspherical particles include singlets (egg-like or ellipsoidal particles), doublets (pear-shaped, dumbbell, or mushroom-like particles), and triplets (ice cream cone-like, popcorn-like, triple rod, diamond-like, or colloidal molecules NH<sub>3</sub> and H<sub>2</sub>O-like particles) [1, 2, 8–15].

In addition, it is also possible to synthesize nonspherical polymer particles via the seeded soap-free emulsion polymerization by crosslinking the second-stage polymer (using linear seed particles), as first reported in our previous article [16]. Submicron-sized poly(methyl methacrylate)/poly(styrene-co-divinylbenzene) [PMMA/P(St-co-DVB)] particles which have multiple dents on particle surface have been successfully synthesized by controlling the amount of styrene monomer and the concentration of DVB crosslinker. If the micron-sized seed particles were used,

S. Shi (✉) · T. Wang · L. Bian · L. Zhao  
Key Laboratory of Applied Technology of Polymer Materials,  
College of Materials Science and Engineering, Shenyang  
University of Chemical Technology, Shenyang 110142, China  
e-mail: sshi@syuct.edu.cn

L. Zhou · S. Kuroda (✉)  
Department of Production Science and Technology,  
Faculty of Engineering, Gunma University, Ota 373-0057, Japan  
e-mail: skuroda@gunma-u.ac.jp

the particles having bowl-like morphology can also be easily obtained [17]. In this article, the seeded soap-free emulsion copolymerization of St with its crosslinker DVB was further studied in the presence of the submicron-sized spherical PMMA seed particles. The effects of the polymerization temperature, the monomer addition mode, and the molecular weight of the PMMA seed on the particle morphology, as well as the polymerization kinetics and morphological evolution, were investigated in detail. Finally, the mechanism for the formation of nonspherical morphology was also proposed.

## Experimental

### Materials

Methyl methacrylate (MMA) monomer was purified by distillation under reduced pressure in a nitrogen atmosphere. St monomer and DVB (55% meta and para isomers) crosslinker were purified by washing repeatedly with 5% aqueous NaOH solution and water, then drying over anhydrous  $\text{Na}_2\text{SO}_4$ , and finally, distilling under a reduced pressure of nitrogen. Potassium persulfate (KPS) initiator was recrystallized from water. The inhibitor-free St and DVB were stored under nitrogen at about  $-10^\circ\text{C}$  until used. DVB and 1-butanethiol (BT, used as a chain transfer agent) were purchased from Sigma-Aldrich. All other reagents were supplied by Wako Pure Chemical Industries. Double-distilled water was used in all experiments.

### Preparation of PMMA seed particles

PMMA seed latex particles were prepared by soap-free emulsion polymerization [18, 19]. To a 300 mL round bottom flask equipped with a mechanical marine-type agitator, a nitrogen inlet and a syringe for sampling, prescribed amounts of MMA, KPS, water, and BT (if used) were added. The mixture was purged with nitrogen for 30 min under stirring (300 rpm) and then heated to  $70^\circ\text{C}$  to initiate the soap-free emulsion polymerization. The polymerization was performed for 6 h, when the monomer conversion usually achieved 96% or more. The obtained

PMMA seed latexes were dialyzed against water for 3 days. The dialysate was changed every 12 h. The detailed polymerization recipes for the preparation of PMMA seed latex particles are given in Table 1.

### Preparation of PMMA/P(St-co-DVB) particles

PMMA/P(St-co-DVB) particles were prepared by seeded soap-free emulsion copolymerization of St and DVB in the presence of PMMA seed particles. The appropriate amounts of PMMA seed latex, water, and KPS were charged into the flask (identical with that used for seed preparation) and purged with nitrogen for 30 min with stirring constantly at 300 rpm. Then, the flask was immersed into the water bath thermostated at the given temperature, and the oxygen-free monomer mixture of St and DVB were added into the flask either batchwise or continuously. For batch monomer addition mode, the flask was sealed immediately after the charge of monomer mixture. The polymerization was carried out for 4 h. For continuous monomer addition mode, the monomer mixture was fed to the flask over different periods of time using a microfeeder. The polymerization was further performed for 4 h after the completion of monomer addition. In all seeded soap-free emulsion copolymerizations, the content of DVB, used as a crosslinker, was held constant at 4.9 wt% based on the St monomer.

### Characterization

#### *Fourier transform infrared spectroscopy (FT-IR)*

FT-IR spectra for the freeze-dried PMMA and PMMA/P(St-co-DVB) particles were obtained on a JASCO FT/IR-8000 spectrometer using the pressed-KBr-pellet method. The specimens for the measurements, with a diameter of 3 mm, were prepared using a Micro KBr Pellet Die (JASCO Parts Center).

#### *Gel permeation chromatography (GPC)*

The number-average molecular weight ( $M_n$ ) and weight-average molecular weight ( $M_w$ ) of the PMMA seed particles

**Table 1** Polymerization recipes and characteristics of the PMMA seed particles

No.	MMA (g)	BT (wt%) <sup>a</sup>	KPS (g)	H <sub>2</sub> O (g)	$D_n$ (nm)	$D_w$ (nm)	$D_w/D_n$	$M_n$ (g/mol)	$M_w$ (g/mol)	$M_w/M_n$
1	30	0	0.16	170	413	415	1.005	$1.2 \times 10^5$	$4.4 \times 10^5$	3.7
2	30	0.25	0.16	170	426	427	1.002	$1.7 \times 10^4$	$4.7 \times 10^4$	2.8
3	30	0.5	0.16	170	429	430	1.002	$1.0 \times 10^4$	$2.5 \times 10^4$	2.5
4	30	1.0	0.16	170	478	479	1.002	$6.7 \times 10^3$	$1.7 \times 10^4$	2.5
5	30	2.0	0.16	170	493	497	1.008	$3.9 \times 10^3$	$8.9 \times 10^3$	2.3

<sup>a</sup> Based on the amount of MMA monomer

were measured by GPC using a TOSOH column ( $\text{TSK}_{\text{gel}}$  GMH<sub>HR</sub>-M) and a differential refractometer (RI-8020). Tetrahydrofuran (THF) was used as eluent at a flow rate of 1.0 mL/min. The calibration curves for GPC analysis were obtained from five linear polystyrene samples ( $M_w = 4.74 \times 10^2$ – $7.75 \times 10^5$  g/mol,  $M_w/M_n = 1.01$ – $1.20$ ).

#### X-ray photoelectron spectroscopy (XPS)

XPS analysis was performed on a Perkin Elmer ESCA 5600 spectrometer with a MgK $\alpha$  X-ray source (1253.6 eV) that was operated at an anode voltage of 15 kV and anode power of 400 W. Pass energies of 187.85 and 58.70 eV with corresponding energy step of 1.60 and 0.25 eV were used for the survey and multi measurements, respectively. All the measurements were made with an analysis area of approximately 800  $\mu\text{m}$  in diameter and at a take-off angle of 45°. The carbon and oxygen atomic concentrations (at.%) were determined from peak-areas of C 1s and O 1s, after correcting with the appropriate sensitivity factors (C, 17.059; O, 41.068). The freeze-dried PMMA/P(St-co-DVB) particles were used for XPS measurements.

#### Field emission scanning electron microscopy (FE-SEM)

The PMMA and PMMA/P(St-co-DVB) particles were observed by FE-SEM (JEOL, JSM-6700F). For PMMA particles, a droplet of the latex, after being sufficiently diluted with water, was dropped onto the double-sided carbon tape and dried in a desiccator at ambient temperature. For PMMA/P(St-co-DVB) particles, the freeze-dried particles were directly placed onto the double-sided carbon tape. All samples were sputter-coated with gold (150 Å) before the FE-SEM observation. By counting at least 100 individual particles from the FE-SEM images, the number-average diameter ( $D_n$ ) and weight-average diameter ( $D_w$ ) of PMMA seed particles were calculated according to the following equations:

$$D_n = \frac{\sum n_i D_i}{\sum n_i}$$

$$D_w = \frac{\sum n_i D_i^4}{\sum n_i D_i^3}$$

where  $n_i$  is the number of PMMA particles with diameter  $D_i$ .

#### Transmission electron microscopy (TEM)

The internal morphology of PMMA/P(St-co-DVB) particles was observed by TEM (JEOL, JEM-1200EXII) on the ultrathin cross-sections. The PMMA/P(St-co-DVB) latexes were coagulated by centrifugation and vacuum-dried. Two

or three pieces of the dried solid chips were embedded in epoxy (EPON 812 resin kit, TAAB) and then the epoxy was cured at 60 °C for 24 h. The cured blocks were trimmed and microtomed using the ultramicrotome supernova (JEOL, JUM-7) with a procedure similar to that described in the literature [20]. The obtained ultrathin cross-sections (ca. 60 nm in thickness) were collected on a carbon-coated micro grid, dried in open air, and exposed to the ruthenium tetroxide ( $\text{RuO}_4$ ) vapor for 3 h at 25 °C. The  $\text{RuO}_4$ -stained ultrathin cross-sections were observed by TEM at an accelerating voltage of 80 kV.

## Results and discussion

### PMMA seed particles

Five series of PMMA seed particles were prepared by soap-free emulsion polymerization under the conditions listed in Table 1. Different concentrations of BT, a chain transfer agent, were added to control the molecular weight of the PMMA seed polymers. As it is clear from Table 1, the  $M_n$  was varied from  $1.2 \times 10^5$  to  $3.9 \times 10^3$  g/mol, decreasing with increasing the concentration of BT from 0 to 2.0 wt%. The FE-SEM images of these particles are given in Fig. 1. The prepared PMMA seed particles were all perfectly spherical with featureless smooth surface. The particle sizes ( $D_n$ ) were in the range of 410–500 nm with very good monodispersity ( $D_w/D_n = 1.002$ – $1.008$ ). Because of the high monodispersity of the particle size, these particles tended to arrange regularly during drying, forming the colloidal crystals in 2 or 3 dimensions.

### Kinetic study of the seeded soap-free emulsion copolymerization

The prepared PMMA particles were used as seeds for the soap-free emulsion copolymerization of St with DVB under various conditions. To investigate the polymerization kinetics, reaction mixture of 1.5 mL was withdrawn from the reactor at various time intervals and immediately freeze-dried. The freeze-dried PMMA/P(St-co-DVB) particles were then analyzed by FT-IR. Figure 2a shows the representative FT-IR spectra of PMMA/P(St-co-DVB) and PMMA particles. A very sharp absorption peak appeared near 700  $\text{cm}^{-1}$  in the spectrum of PMMA/P(St-co-DVB) as compared with that of PMMA. This peak could be reasonably assigned to the characteristic absorption of aromatic C–H bending vibration, indicating that PS component had been successfully introduced into the PMMA seed particles. The PS content in PMMA/P(St-co-DVB) particles (relative to PMMA) was quantified by the absorbance ratio of the peak at 700  $\text{cm}^{-1}$  (for PS) to that at 1375  $\text{cm}^{-1}$  (CH<sub>3</sub> bending, for

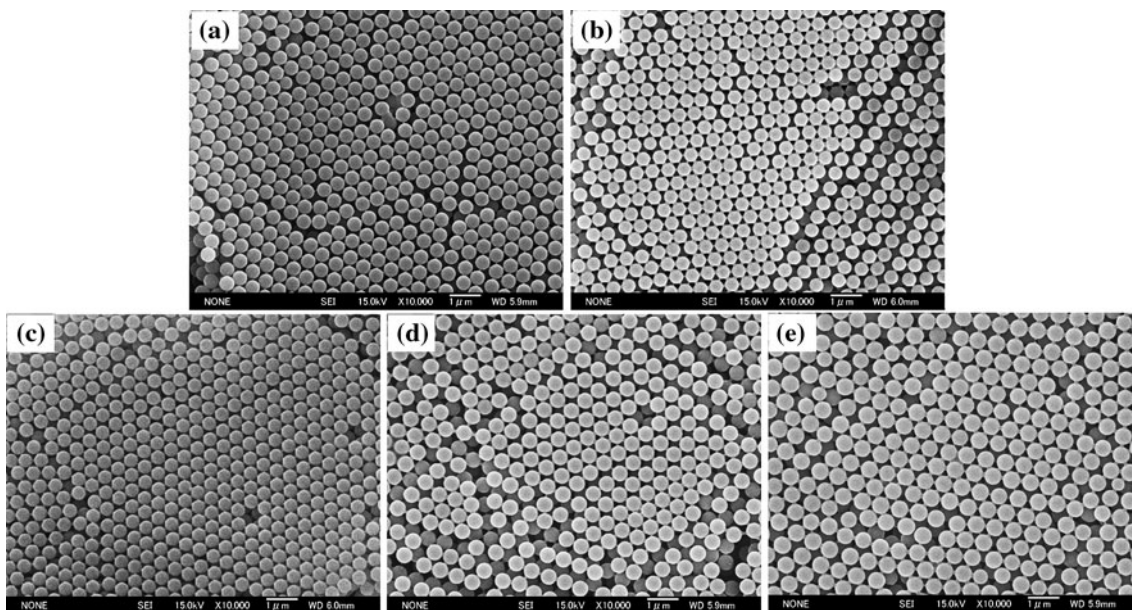


**Fig. 1** FE-SEM images of the PMMA seed particles prepared by soap-free emulsion polymerization with different concentrations of BT: **a** 0 wt%, **b** 0.25 wt%, **c** 0.5wt%, **d** 1.0 wt%, and **e** 2.0 wt%

PMMA), with a calibration curve obtained from the mixture of PMMA and PS latex particles. From the PS content, the monomer conversion was calculated [21]. Figure 2b displays a representative plot of monomer conversion versus polymerization time. It is clear that the monomer conversion increased almost linearly with the polymerization time and the polymerization completed within 1 h. The final monomer conversion was about 93%.

#### Evolution of nonspherical PMMA/P(St-co-DVB) particles during seeded soap-free emulsion copolymerization

The seeded soap-free emulsion copolymerization of St and DVB, the kinetic data of which had been shown in Fig. 2b

eventually led to the formation of nonspherical multidentated PMMA/P(St-co-DVB) particles. The FE-SEM images for the PMMA/P(St-co-DVB) particles sampled at different polymerization times are shown in Fig. 3. At the early stage of polymerization, the obtained PMMA/P(St-co-DVB) particles were spherical (Fig. 3a, b). As the polymerization proceeded to 15 min (25.4% monomer conversion), the size of resultant particles increased to some extent but the particles still maintained their sphericity (Fig. 3c). However, at the polymerization time of 20 min (38.8% monomer conversion), the particles with slightly deformed surface were observed (Fig. 3d). As the polymerization further progressed to 30, 40, and 50 min (55.9, 73.4, and 87.9% monomer conversions), the particle surface became more and more deformed (Fig. 3e–g). Finally, when the polymerization was

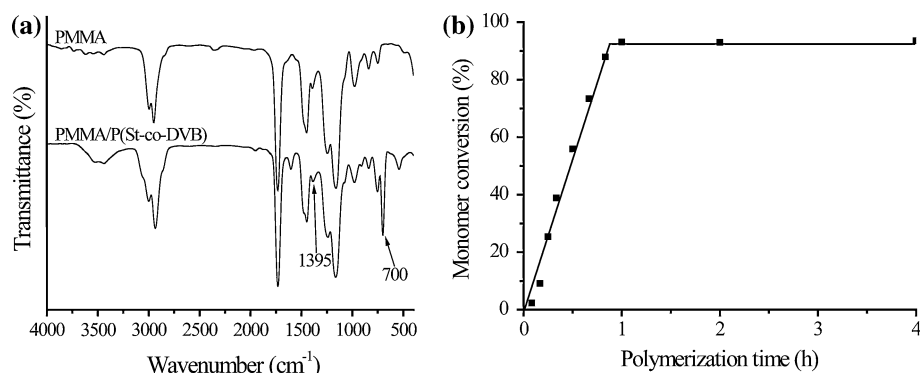


**Fig. 2** **a** The typical FT-IR spectra of PMMA (0 wt% BT) and PMMA/P(St-co-DVB) particles, and **b** the plot of monomer conversion versus polymerization time for the synthesis of PMMA/P(St-co-DVB) particles by seeded soap-free emulsion copolymerization.

Polymerization conditions: PMMA seed (0 wt% BT) = 0.6 g, St = 1.46 g, DVB = 4.9 wt%, KPS = 0.02 g, H<sub>2</sub>O = 130 mL, temperature = 60 °C, batch monomer addition mode

completed (ca. 93.2% monomer conversion), the PMMA/P(St-co-DVB) particles with multiple dents on the surface were formed (Fig. 3h, i).

On the other hand, the solubility experiment of the resulted particles in THF, a good solvent for both PS and PMMA, showed that a 3D network had effectively formed from the polymerization time of 15 min (the particles became insoluble in the solvent). This suggests that the formation of the dented PMMA/P(St-co-DVB) particles was a direct result of the formation of the 3D crosslinked network in the particles during the seeded soap-free emulsion copolymerization.

#### Influence of polymerization temperature on particle morphology

It was found that the polymerization temperature had a great effect on the surface morphology of PMMA/P(St-co-DVB) particles in the seeded soap-free emulsion copolymerizations of St and DVB on the PMMA seed particles. The polymerization temperatures were varied from 60 to

80 °C, while maintaining other conditions unchanged. The polymerization at 60 °C, in which no samples were withdrawn from the reactor during polymerization, was a control experiment for that studying the polymerization kinetics and morphological evolution described above. The FE-SEM images for the PMMA/P(St-co-DVB) particles obtained in this set of experiments are shown in Fig. 4. It is evident that the polymerization at 60 °C produced highly dented PMMA/P(St-co-DVB) particles (Fig. 4a). In contrast, the polymerizations at both 70 and 80 °C resulted in the particles having normal smooth surface (Fig. 4b, c).

#### Influence of monomer addition mode on particle morphology

In all the seeded soap-free emulsion copolymerizations described above, the second-stage monomers were charged to the reactor batchwise. In addition, we also performed the polymerization using continuous monomer addition mode at various monomer feed rates. The mixture of St and DVB was fed to the reactor over 10, 20, 30, and 60 min. The

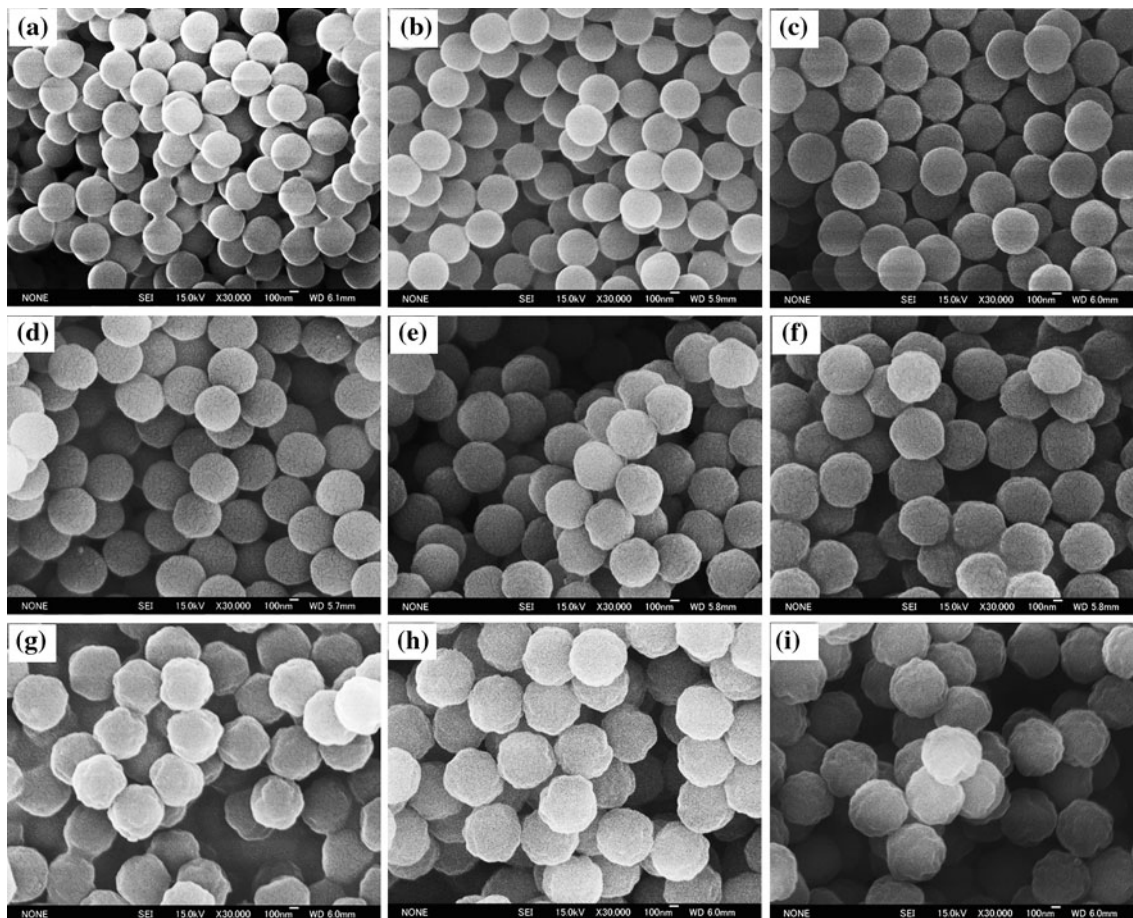


**Fig. 3** FE-SEM images of the PMMA/P(St-co-DVB) particles sampled at different polymerization times: **a** 5 min, **b** 10 min, **c** 15 min, **d** 20 min, **e** 30 min, **f** 40 min, **g** 50 min, **h** 60 min, and **i** 240 min.

Polymerization conditions: PMMA seed (0 wt% BT) = 0.6 g, St = 1.46 g, DVB = 4.9 wt%, KPS = 0.02 g, H<sub>2</sub>O = 130 mL, temperature = 60 °C, batch monomer addition mode

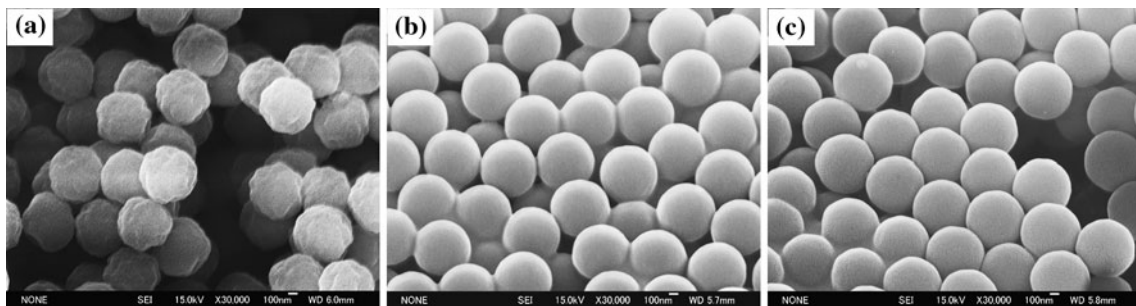


**Fig. 4** FE-SEM images of the PMMA/P(St-co-DVB) particles prepared at different polymerization temperatures: **a** 60 °C, **b** 70 °C, and **c** 80 °C. Polymerization conditions: PMMA seed

(0 wt% BT) = 0.6 g, St = 1.46 g, DVB = 4.9 wt%, KPS = 0.02 g, H<sub>2</sub>O = 130 mL, monomer conversion = 93 ± 3%, batch monomer addition mode

FE-SEM images of resulting PMMA/P(St-co-DVB) particles are given in Fig. 5. The FE-SEM image of Fig. 5a was for the control experiment using batch monomer addition mode, which showed the heavily dented PMMA/P(St-co-DVB) particles as expected. In contrast, the polymerizations using continuous monomer addition mode produced the particles having less deformed surface. The deformation extent of the particle surface decreased as the monomer feed time increased from 10 min to 30 min (Fig. 5b–d). At the monomer feed time of 60 min, the normal spherical particles with smooth surface were obtained (Fig. 5e).

In seeded polymerization using continuous monomer addition mode, a starve-fed condition can be achieved if the monomer is fed to the reactor at a sufficiently slow rate. The kinetics of the seeded soap-free emulsion polymerization at monomer feed time of 60 min was investigated, and the result is presented in Fig. 6. It is evident that the monomer conversion line was essentially parallel to the monomer feed line, a characteristic of a starve-fed polymerization [22]. As shown in Fig. 5e, the starve-fed seeded soap-free emulsion copolymerization of St and DVB resulted in the smooth-surfaced particles.

#### Influence of molecular weight of PMMA seed on particle morphology

As introduced previously, we prepared five kinds of PMMA seed particles having different molecular weights by varying the concentration of BT in the soap-free emulsion polymerization of MMA. The PMMA particles that possessed the highest molecular weight ( $M_n = 1.2 \times 10^5$  g/mol, BT = 0 wt%) were used in all the seeded soap-free emulsion copolymerizations discussed above. In this study, the effect of molecular weight of PMMA seed particles on the particle morphology was also investigated, and the results are given in Fig. 7. In this set of experiments, except for the kind of PMMA seed particles, all other parameters were left constant. Batch monomer addition mode was adopted. In

comparison with the highly distorted PMMA/P(St-co-DVB) particles obtained using PMMA seed of 0 wt% BT, the particles obtained using PMMA seed of 0.25 wt% BT ( $M_n = 1.7 \times 10^4$  g/mol) appeared less distorted (Fig. 7a, b). Further increasing the concentration of BT to 0.5 and 1.0 wt%, which reduced the  $M_n$  to  $1.0 \times 10^4$  and  $6.7 \times 10^3$  g/mol, led to the PMMA/P(St-co-DVB) particles with circular indentations on their surface (Fig. 7c, d). The number of these indentations tended to decrease as the concentration of BT increased. Finally, at BT concentration of 2.0 wt%, the normal spherical PMMA/P(St-co-DVB) particles were prepared (Fig. 7e). In addition, some new particles with much smaller size were inevitably formed when PMMA seed particles of relatively low molecular weight were used.

The internal morphology of PMMA/P(St-co-DVB) particles obtained in this set of experiments was examined by TEM on the ultrathin cross-sections. The corresponding TEM images are given in Fig. 8. It is obvious that all PMMA/P(St-co-DVB) particles showed a typical core/shell structure. The dark P(St-coDVB)-rich phase formed the shell encasing the bright PMMA-rich core. In particular, at higher BT concentrations of 1.0 and 2.0 wt%, some small P(St-co-DVB) phases of ca. 30 nm in diameter were observed in the region of PMMA-rich core, as shown in Fig. 8c, d. The amount of these small P(St-co-DVB) phase seemed to increase as the BT concentration increased.

In the present seeded soap-free emulsion copolymerization, the internal morphology of the resulting particles is determined by the combined effect of particle/water interfacial tension and local viscosity of polymerization loci at reaction temperature, the former acting as thermodynamic factor and the latter as kinetic factor [23]. During the seeded soap-free emulsion copolymerization, the newly formed second-stage P(St-co-DVB) polymer would show a strong tendency to penetrate into the interior of PMMA seed particle (and vice versa) so as to form the relatively hydrophilic PMMA/water interface instead of hydrophobic P(St-co-DVB)/water interface. The extent of this phase migration mainly depended on the internal particle

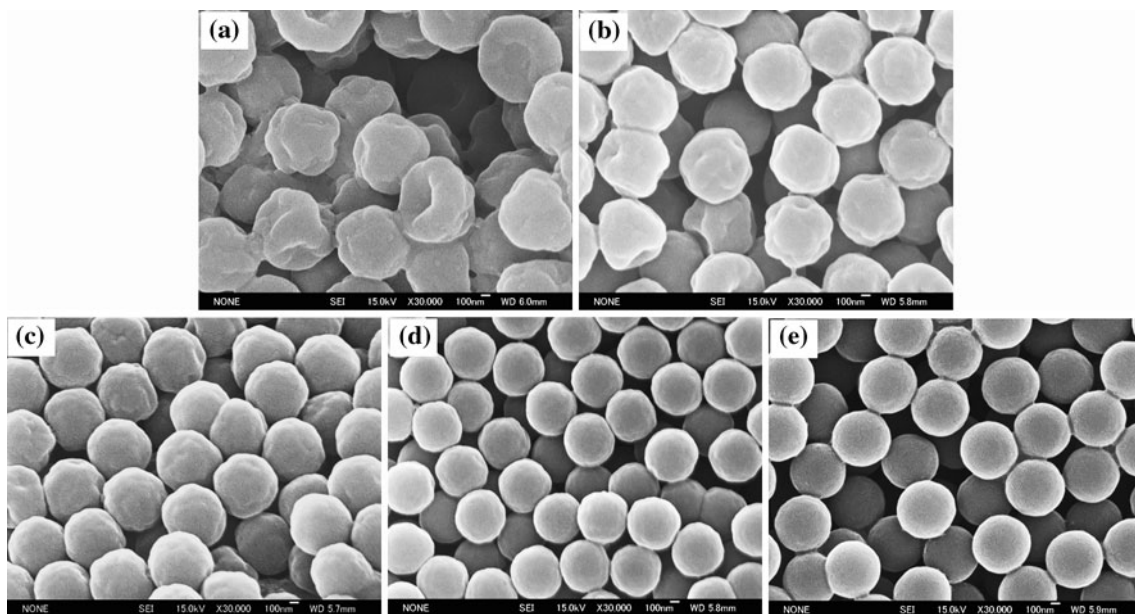


**Fig. 5** FE-SEM images of the PMMA/P(St-co-DVB) particles prepared using batch monomer addition mode **a** and continuous monomer addition mode at different feeding times: **b** 10 min, **c** 20 min, **d** 30 min, and **e** 60 min. Polymerization conditions:

PMMA seed (0 wt% BT) = 1.2 g, St = 4.4 g, DVB = 4.9 wt%, KPS = 0.08 g, H<sub>2</sub>O = 130 mL, temperature = 60 °C, monomer conversion = 87 ± 8%

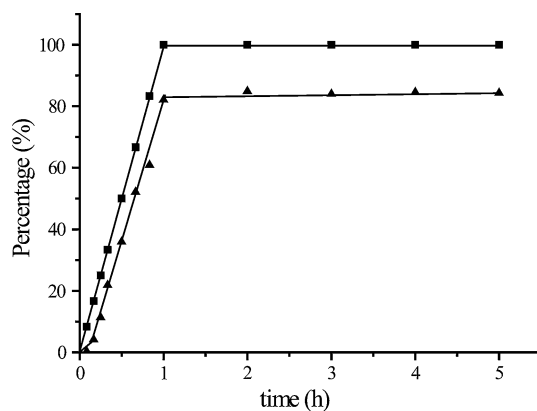


**Fig. 6** Plots of the monomer conversion (triangle) and the fraction of the monomer that had been fed to the flask (square) versus time for the seeded soap-free emulsion copolymerization. Polymerization conditions: PMMA seed (0 wt% BT) = 1.2 g, St = 4.4 g, DVB = 4.9 wt%, KPS = 0.08 g, H<sub>2</sub>O = 130 mL, temperature = 60 °C, monomer feeding time = 60 min

viscosity, which closely relates to the molecular weight of seed particles [24]. The smaller the molecular weight, the lower the intraparticle viscosity, and the easier the P(St-co-DVB) phase migrated into the particle interior. Accordingly, though most P(St-co-DVB) phase was located on the particle periphery, some had penetrated into the particle interior in the cases that PMMA seed particles of relatively low molecular weight were used, as shown in Fig. 8c, d. On the other hand, the atomic concentrations of carbon and

oxygen on the top surface of PMMA/P(St-co-DVB) particles were investigated by XPS, and the results are listed in Table 2. Although no appreciable difference was observed in the P(St-co-DVB)-rich shell from the TEM images, the concentration of oxygen atom, which originates mainly from the PMMA, increased as the concentration of BT increased. At 2.0 wt% BT concentration, the concentration of oxygen was almost two times than that of 0 wt% BT concentration. This indicates that more PMMA chains diffused to the particle surface when the molecular weight of PMMA seed particles decreased.

#### Formation mechanism of the dented PMMA/P(St-co-DVB) particles

The formation of the dented PMMA/P(St-co-DVB) particles was attributed to the elastic force introduced by crosslinking the second-stage polymer in the seeded soap-free emulsion copolymerization. As the polymerization proceeded to certain extent, P(St-co-DVB) 3D network developed around the original PMMA seed particles. The formed P(St-co-DVB) network, which was still growing, was proposed to swell by absorbing the unreacted monomers and then contract to relax the polymer chains [13, 25]. However, the uneven crosslinking structure of the 3D network provoked phase separation of St and DVB monomers (and possibly some linear PMMA and PS chains) from the denser regions to the looser regions of the crosslinked network [26]. As monomer conversion further

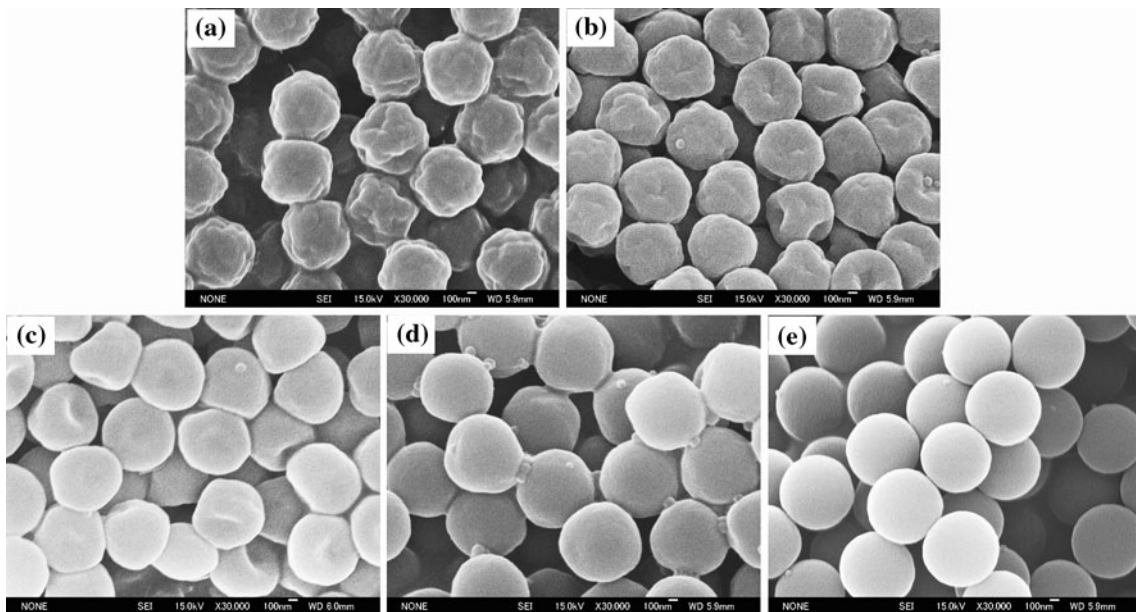


**Fig. 7** FE-SEM images of the PMMA/P(St-co-DVB) particles prepared using PMMA seed particles of different BT concentrations: **a** 0 wt%, **b** 0.25 wt%, **c** 0.5 wt%, **d** 1.0 wt%, and **e** 2.0 wt%. Polymerization conditions: PMMA seed = 0.6 g, St = 1.80 g, DVB = 4.9 wt%, KPS = 0.02 g, H<sub>2</sub>O = 130 mL, temperature = 60 °C, monomer conversion = 89 ± 5%, batch monomer addition mode

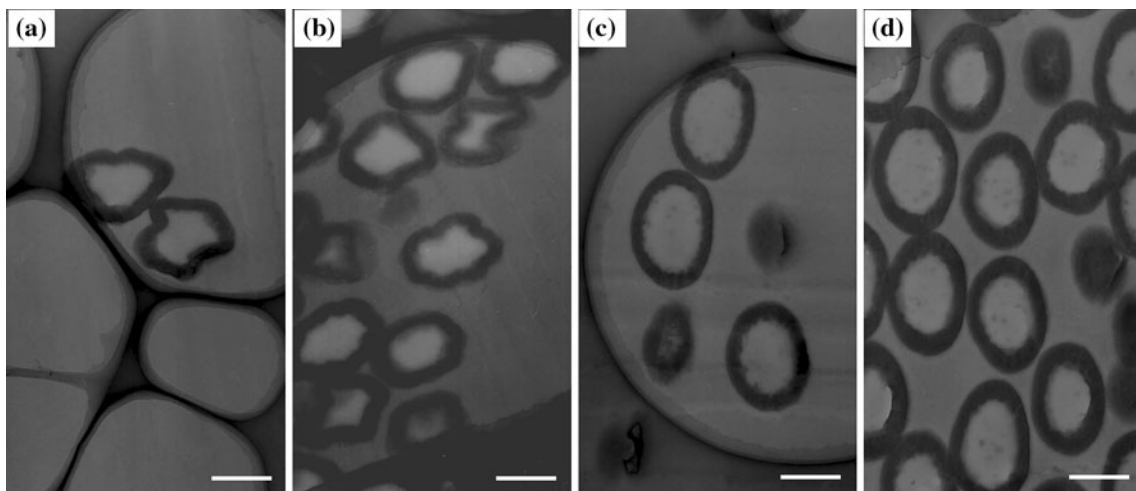


**Fig. 8** TEM images of the ultramicrotomed PMMA/P(St-co-DVB) particles prepared using PMMA seed particles of different BT concentrations: **a** 0 wt%, **b** 0.25 wt%, **c** 1.0 wt%, and **d** 2.0 wt%. P(St-co-DVB) phase was stained dark with RuO<sub>4</sub> vapor. Scale bars:

400 nm. Polymerization conditions: PMMA seed = 0.6 g, St = 1.80 g, DVB = 4.9 wt%, KPS = 0.02 g, H<sub>2</sub>O = 130 mL, temperature = 60 °C, monomer conversion = 89 ± 5%, batch monomer addition mode

increased, PMMA/P(St-co-DVB) particles with multiple dents on their surface were eventually formed.

During this process, the presence of monomers, which had not yet participated in polymerization, was necessary for the phase separation caused by the swelling and contracting of the uneven 3D network. Therefore, the starved seeded soap-free emulsion copolymerization led to the formation of normal spherical PMMA/P(St-co-DVB) particles, as shown in Fig. 5. To prepare the dented particles, it was also essential to form a relatively “pure”

**Table 2** Carbon and oxygen atomic concentrations on the surface of PMMA/P(St-co-DVB) particles obtained by XPS measurement

No.	BT (wt%)	C 1s at.%	O 1s at.%
1	0	86.6	13.4
2	0.25	85.1	14.9
3	0.5	84.4	15.6
4	1.0	79.2	20.8
5	2.0	75.8	24.2

P(St-co-DVB) 3D network on the particle surface so that the elastic force can dominate the surface tension, which is known to favor the spherical particle. When more linear PMMA chains were present on the particle surface, the particles would preferentially grow to the spherical ones under the effect of the surface tension, as shown in Fig. 7. On the other hand, the degree of phase separation was reduced by elevating the polymerization temperature, giving the normal spherical particles at 70 and 80 °C, as shown in Fig. 4. We cannot yet provide very satisfactory explanation about this phenomenon at present. However, the kinetic study showed that the higher temperature brought about the higher polymerization rate (not shown for brevity). It was speculated that, at higher temperature, the polymerization probably tended to finish before phase separation occurred because the contracting of a crosslinked network upon swelling is a somewhat time-consuming process [13]. As a result, the spherical PMMA/P(St-co-DVB) particles with smooth surface were obtained.

## Conclusion

We demonstrated the preparation of nonspherical dented PMMA/P(St-co-DVB) particles by seeded soap-free emulsion copolymerization of St and DVB in the presence of spherical linear PMMA particles. Various polymerization parameters such as polymerization temperature, monomer addition mode, and molecular weight of PMMA seed were found to influence the particle morphology. The generation of such nonspherical particles was ascribed to the formation of uneven crosslinked network during the seeded soap-free emulsion copolymerization.

**Acknowledgements** This study was supported in part by the National Natural Science Foundation of China (No.50943028), the Scientific Research Foundation for the Returned Overseas Chinese Scholars of State Education Ministry, and the Scientific Research Foundation of Education Department of Liaoning Province (No.2008T155).

## References

1. Yang M, Wang G, Ma HT (2011) Chem Comm 47:911
2. Kim JW, Larsen RJ, Weitz DA (2007) Adv Mater 19:2005
3. Park JG, Forster JD, Dufresne ER (2010) J Am Chem Soc 132:5960
4. Shi S, Zhou LM, Wang T, Bian LN, Tang YT, Kuroda S (2011) J Appl Polym Sci 120:501
5. Wang HG, Liu QW, Yang QB, Li YC, Wang W, Sun L, Zhang CQ, Li YX (2010) J Mater Sci 45:1032. doi:[10.1007/s10853-009-4035-1](https://doi.org/10.1007/s10853-009-4035-1)
6. Goodall AR, Wilkinson MC, Hearn J (1977) J Polym Sci Polym Chem Ed 15:2193
7. Durant YG, Sundberg EJ, Sundberg DC (1997) Macromolecules 30:1028
8. Tang C, Zhang CL, Liu JG, Qu XZ, Li JL, Yang ZZ (2010) Macromolecules 43:5114
9. Park JG, Forster JD, Dufresne ER (2009) Langmuir 25:8903
10. Shi S, Kuroda S, Kubota H (2003) Colloid Polym Sci 281:331
11. Shi S, Wang T, Tang YT, Zhou LM, Kuroda S (2011) Chinese Chem Lett. doi:[10.1016/j.cclet.2011.04.018](https://doi.org/10.1016/j.cclet.2011.04.018)
12. Nagao D, Kats CM, Hayasaka K, Sugimoto M, Konno M, Imhof A, Blaaderen A (2010) Langmuir 26:5208
13. Sheu HR, El-aasser MS, Vanderhoff JW (1990) J Polym Sci Polym Chem 28:629
14. Kim JW, Larsen RJ, Weitz DA (2006) J Am Chem Soc 128: 14374
15. Shin K, Lee S, Kim JJ, Suh KD (2010) Macromol Rapid Commun 31:1987
16. Shi S, Hayami H, Kuroda S, Kubota H (2006) Chem Lett 35:320
17. Wang ZF, Wang T, Bian LN, Zhou LM, Shi S, Kuroda S (2011) Chinese J Polym Sci. doi:[10.1007/s10118-011-1062-6](https://doi.org/10.1007/s10118-011-1062-6)
18. Wang T, Shi S, Akiyama Y, Zhou LM, Kuroda S (2010) J Mater Sci 45:4539. doi:[10.1007/s10853-010-4648-4](https://doi.org/10.1007/s10853-010-4648-4)
19. Cheng XJ, Zhao Q, Yang YK, Tjong SC, Li RKY (2010) J Mater Sci 45:777. doi:[10.1007/s10853-009-4000-z](https://doi.org/10.1007/s10853-009-4000-z)
20. Begum S, Jones IP, Jiao C, Lynch DE, Preece JA (2010) J Mater Sci 45:3697. doi:[10.1007/s10853-010-4479-3](https://doi.org/10.1007/s10853-010-4479-3)
21. Wang T, Shi S, Yang F, Zhou LM, Kuroda S (2010) J Mater Sci 45:3392. doi:[10.1007/s10853-010-4449-9](https://doi.org/10.1007/s10853-010-4449-9)
22. Stubb JM, Sundberg DC (2006) J Appl Polym Sci 102:945
23. Shi S, Kuroda S, Tadaki S, Kubota H (2002) Polymer 43:7443
24. Karlsson OJ, Hassander H, Wesslén B (2000) J Appl Polym Sci 77:297
25. Sperling LH (2001) Introduction to physical polymer science, 3rd edn. Wiley-interscience, New York
26. Thomson B, Rudin A, Lajoie G (1996) J Appl Polym Sci 59:2009